Telechelic Poly(*N*-isopropylacrylamides) via Nitroxide-Mediated Controlled Polymerization and "*Click*" Chemistry: Livingness and "*Grafting-from*" Methodology

Wolfgang H. Binder,*,† Dietrich Gloger,† Harald Weinstabl,† Günther Allmaier,‡ and Ernst Pittenauer‡

Makromolekulare Chemie, Martin-Luther Universität Halle-Wittenberg, Heinrich-Damerow Strasse 4, D-06120 Halle (Saale), Germany, Institute of Chemical Technologies and Analytics, Vienna University of Technology, 1060 Vienna, Austria

Received December 12, 2006; Revised Manuscript Received March 14, 2007

ABSTRACT: We report on the synthesis of telechelic poly(*N*-isopropylacrylamides) (PNIPAM) via nitroxide-mediated controlled polymerization, putting a focus on the introduction of defined end group moieties into telechelic poly(*N*-isopropylacrylamide) and poly(*n*-butyl acrylates). Various functional groups, linked to the central nitroxide-initiator via a triazole moiety resulting from an azide/alkyne-"click" reaction were probed with *N*-isopropylacrylamide and *n*-butyl acrylate as monomers in terms of efficiency and livingness. Functional groups on the initiator include a 1,2-dihydroxyalkyl moiety and a barbituric acid moiety as well as a phenyl moiety. Those initiators with a 1,2,3-1*H*-triazole moiety directly bound to the initiator group displayed a poor initiating quality toward *N*-isopropylacrylamide, whereas an ester bridge as linker between the initiator molecule and the functional group showed highly living character with respect to *N*-isopropylacrylamide and *n*-butyl acrylate as probed by kinetic experiments. Effects based upon internal hydrogen-bonding effects are made responsible rather than purely stereoelectronic effects, as proven by force-field calculations. MALDI time-of-flight mass spectrometry was used to prove the incorporation of the respective end groups into the telechelic PNIPAM polymers. Finally, the versatility of the method was demonstrated via a "grafting-from" approach of PNIPAM from magnetic iron oxide nanoparticles via a surface-bound initiator, resulting in an excellent control of molecular weight and thus thickness of the polymeric shell around the magnetic nanoparticles.

Introduction

The synthesis of well-defined poly(*N*-isopropylacrylamides) (PNIPAM),[1] characterized by a defined chain length and the presence of functional end groups, as well as a low polydispersity still represents a major point of interest. Because of PNIPAM's coil/globule transition at moderate temperatures (30−45 °C) this polymer has found wide application in various temperature- and solvent triggered systems, such as in modulative capsules,[2] as switchable valves in microfluidic systems and surfaces,[3] as responsive surfaces regulating cell detachment,[4] or within thermoresponsive materials.[5] Besides the free radical polymerization processes of *N*-isopropylacrylamide (NIPAM), several controlled polymerization processes such as RAFT and ATRP have been probed for the preparation of defined PNIPAM-polymers, resulting in a multitude of different telechelic polymers. As the RAFT polymerization process of NIPAM has been described extensively, the possibility to modify functional groups via the trithiocarbonate[6−8] or dithioate[9−13] linkages is limited to sulfide-exchange reactions with appropriate thiols and sulfide-addition reactions onto functionalized maleimides. Using this strategy, postfunctionalization reactions with fluorescent-pyrene labels and alkyl moieties have been described. Recently, ATRP has been investigated as a method for the polymerization of NIPAM,[14,15] resulting in telechelic PNIPAM polymers with polydispersities below 1.2 by use of chloropropionates as initiators and the couple $Cu^{I}Cl$/tris[2-(dimethylamino)ethyl]amine as catalytic system. In addition to phenyl groups, the preparation of a biotinylated PNIPAM derivatives[16] has been described. Surface-initiated polymerization reactions of NIPAM via ATRP have been described extensively,[17−26] often demonstrating the thickness increase with progress of the polymerization reaction.

As seen from the limited amount polymerization methods in solution resulting in telechelic PNIPAM polymers, the nitroxide-mediated controlled polymerization (NMP)[27,28] of NIPAM represents an important alternative for the preparation of well-defined PNIPAM polymers. First reports on NIPAM polymerization via NMP date back to a publication of Hawker et al. in 2001[29] based on the use of α-hydrogen containing nitroxides such as 2,2,5-trimethyl-3-(phenylethoxy)-4-phenyl-3-azahexane (TIPNO-styryl),[30] followed by a more detailed account in 2003,[31] mentioning NIPAM as monomer only on the side with polydispersities below 1.1 of the resulting PNIPAM polymers. Subsequent investigations[32] with the same initiator under copolymerization conditions with NIPAM and *N*-hydroxysuccinimide esters of methacrylic acid resulted in polymers with polydispersities of ∼1.5 and larger. Indeed, a strong dependence on the nitroxide moiety was observed, reporting *N*-*tert*-butyl-*N*-[1-diethylphosphono-(2,2-dimethylpropyl)]nitroxide[33] (PD ∼1.2−1.3) and 2,2,6,6-tetramethylpiperidine-*N*-oxide (TEMPO)[34] (surface initiated NIPAM polymerization with a linear increase of layer thickness with time) as effective initiating systems. Surprisingly, a grafting-from approach of NIPAM, relying on *N*,*N*-di-*tert*-butyl nitroxide as initiating nitroxide[35] only furnished the PNIPAM polymer with a polydispersity of 4.5. A breakthrough in the NMP-process of NIPAM has been reported by Studer et al.,[36] relying on 2,2,6,6-tetraethylpiperidin-4-on-*N*-oxyl as sterically hindered nitroxide within the initiator, resulting

† Makromolekulare Chemie, Martin-Luther Universität Halle-Wittenberg.
‡ Institute of Chemical Technologies and Analytics, Vienna University of Technology.
* Corresponding author. E-mail: wolfgang.binder@chemie.uni-halle.de.

10.1021/ma0628376 CCC: $37.00
Published on Web 04/07/2007

Scheme 1. Structures of the Nitroxide Initiators 1, 2, and 3 for the Polymerization of *N*-Isopropylacrylamide and *n*-Butyl Acrylate

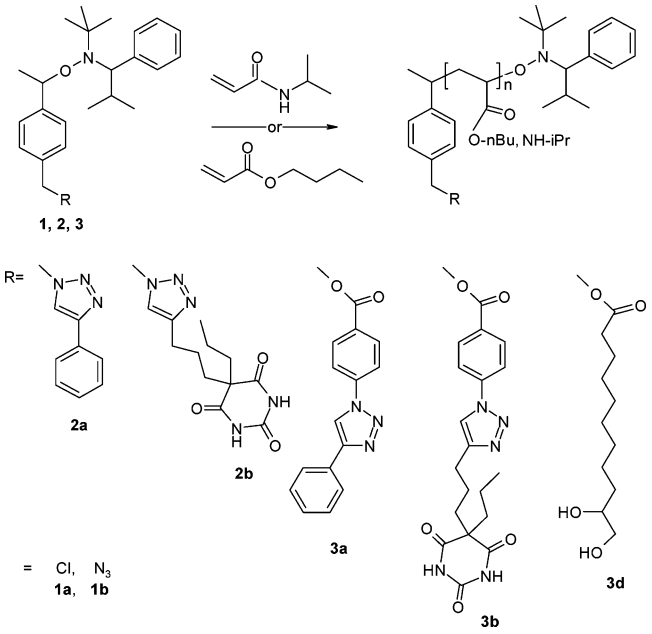

in telechelic polymers with polydispersities below 1.2 as proven by MALDI-analysis. As revealed by these examples, the steric and electronic structure of the nitroxide and the initiating radical can strongly influence the outcome of the NMP-mediated polymerization process, thus resulting in the absence of livingness and controlled polymerization upon even small changes within the initiator structure.

In the present publication, a new approach toward endfunctionalized, telechelic NIPAM polymers via an NMP-mediated polymerization relying on the TIPNO-based initiators **1**, **2**, and **3** is described (see Scheme 1). The basic strategy for the generation of various NMP initiators is based upon a combination of Hawkers 2,2,5-trimethyl-3-(4′-chloromethyl-phenylethoxy)-4-phenyl-3-azahexane initiator **1a**[31] and its 4′-azido-methyl derivative **1b**, from which the azide/alkine-"click" reaction enables the generation of various initiators bearing functional groups **2** and **3**. Main issue of this work concerned the initiating quality of NIPAM using these initiators, as well as the possibility to generate telechelic polymers bearing the corresponding end group moieties bound to the initial initiators **1**−**3**. Moreover, the 1,2-diol-bearing initiator **3d** was used to probe a grafting-from method of NIPAM via NMP methods directly from iron oxide nanoparticles, resulting in the successful generation of magnetic iron oxide core/shell nanoparticles with a defined PNIPAM shell around the nanoparticle.

Experimental Section

General Data. ^{1}H and ^{13}C NMR spectra were recorded at room temperature on a Bruker AC-E-200 (200 MHz) and a Bruker Avance DRX-400 (400 MHz) FT-NMR spectrometer. $CDCl_3$ (Isotec Inc. 99.8 atom% D) and DMSO-d_6 (HDO + D_2O < 0.02%) were used as solvents. Chemical shifts were recorded in parts per million (δ) and referenced to residual protonated solvent ($CDCl_3$, 7.26 ppm (^{1}H) and 77.0 ppm (^{13}C); DMSO-d_6, 2.54 ppm (^{1}H) and 40.45 ppm (^{13}C)). GPC analysis was performed on a Viscothek VE 2001 system using Styragel linear columns linear columns HR0.5, HR3, and HR4 in THF at 40 °C. Polystyrene standards (M_p = 580 − 488400 g/mol) were used for conventional external calibration using a Waters RI 2410 refractive index detector.

Solvents/Reagents. Methanol was dried over CaH_2 refluxing for 24 h hours, distilled and stored with activated Klinosorb 3 Å molecular sieve. Tetrahydrofuran (THF) was refluxed over sodium wires and benzophenone overnight, distilled, and stored with activated Klinosorb 4 Å molecular sieve. Chloroform and dichloromethane were refluxed over K_2CO_3, distilled and stored with activated Klinosorb 4 Å molecular sieves. DMF was refluxed with calcium hydride, distilled, and stored with activated Klinosorb 4 Å molecular sieves. Toluene was refluxed over sodium, distilled and stored with Klinosorb 4 Å molecular sieves. Triethylamine was purchased from Aldrich and refluxed for 2 h over calcium hydride prior to use. Tetrakis(acetonitrile)hexafluorophosphate copper(I), sodium azide, diisopropylethylamine (DIPEA), hexamethylphosphoric acid triamide (HMPA), ethynylbenzene, osmium tetroxide, *N*-methyl morpholine-*N*-oxide (NMO), *N*-ispopropylacrylamide (NIPAM), *n*-butyl acrylate (*n*-BuA), TBTA (tris(benzyltriazolylmethyl)amine), and ethyl vinyl ether were purchased from Aldrich and used as received. 2,2,5-Trimethyl-3-(1′-p-azidomethylphenylethoxy)-4-phenyl-3-azahexane was prepared according to Hawker et al.[30,37]

Synthesis of 2,2,5-Trimethyl-3-(1′-*p*-azidomethylphenylethoxy)-4-phenyl-3- azahexane (1b). 2,2,5-Trimethyl-3-(1′-p-azidomethylphenylethoxy)-4-phenyl-3-azahexane (**1b**) was prepared in close analogy to a procedure reported in the literature,[31] although without the use of a phase transfer catalyst. 2,2,5-Trimethyl-3-(1′-*p*-chloromethylphenylethoxy)-4-phenyl-3-azahexane (**1a**) (200 mg, 0.53 mmol), was dissolved in 5 mL of dry DMF and placed in a one-necked round-bottomed flask. Sodium azide (105 mg, 1.6 mmol) was added with a spatula. NaN_3 dissolved very slowly, and the reaction mixture became cloudy. After the mixture was stirred overnight, a complete conversion of **1a** and the formation of **1b** was observed by TLC, hexane/chloroform, 20:1, R_f = 0.3). The solvent (DMF) was removed in vacuo and the residue was redissolved in dichloromethane to separate (**1b**) from the residual salts. Evaporation of the solvent gave (**1b**) as light-brown gum, yield 98%. Data for **1b**: R_f = 0.3 (hexane/chloroform, 20:1). ^{1}H NMR (200 MHz, $CDCl_3$) (both diastereomers): δ 7.49 (m, 18H, phenyl-H), 4.93 (q, 2H, CH), 4.33 (d, 4H, $-CH_2-N_3$), 3.43 (d, 1H,^3J = 10.71 Hz, CH), 3.30 (d, 1H,^3J = 10.71 Hz, CH), 2.39 (m, 1H, CH), 1.62 (d, 3H,^3J = 6.3 Hz, CH_3),1.53 (d, 3H,^3J = 6.3 Hz, CH_3), 1.4 (m, 1H, CH), 1.26 (d, 3H, CH_3), 1.28 (d, 3H,^3J = 6.3 Hz, CH_3), 1.05 (s, 9H, $NCCH_3$), 0.96 (d, 3H,^3J = 6.3 Hz, CH_3), 0.77 (s, 9H, CH_3), 0.55 (d, 3H,^3J = 6.5 Hz, CH_3), 0.22 (d, 3H,^3J = 6.5 Hz, CH_3)

^{13}C NMR (50 MHz, $CDCl_3$) (both diastereomers): δ 145.8 (phenyl-C), 145.7 (phenyl-C), 142.2 (phenyl-C), 142.1 (phenyl-C), 134.1 (phenyl-C), 133.6 (phenyl-C), 130.9 (phenyl-CH), 130.8 (phenyl-CH), 128.0 (phenyl-CH) , 127.9 (phenyl-CH), 127.4 (phenyl-CH), 127.3 (phenyl-CH), 127.1 (phenyl-CH), 126.6 (phenyl-CH), 126.3 (phenyl-CH), 126.1 (phenyl-CH), 83.10 (CH), 82.40 (CH), 72.10 (CH), 72.00 (CH), 60.50 (C), 60.40 (C) , 54.50 ($-CH_2-N_3$), 54.50 ($-CH_2-N_3$), 31.90 (CH), 31.60 (CH), 28.30 (CH_3), 28.10 (CH_3), 24.50 (CH_3), 23.10 (CH_3), 22.00 (CH_3), 21.80 (CH_3), 21.00 (CH_3), 20.90 (CH_3).

Synthesis of the Initiators 2a, 2b, 3a, and 3b by Sharpless-Type "Click"-Chemistry. All of the click-chemistry reactions were performed under identical conditions with respect to scale, reaction time, and catalyst-system. The alkyne-functionalized moieties were employed in excess with respect to the azido compound.

2,2,5-Trimethyl-(1′-*p*-(4-phenyl-1H-1,2,3-triazol-1-yl)methylphenylethoxy-4-phenyl-3-azahexane (2a). 2,2,5-Trimethyl-3-(1′-p-azidomethylphenylethoxy)-4-phenyl-3-azahexane (**1b**)[31] (70 mg, 0.185 mmol) and ethynylbenzene (**4a**) (37.7 mg, 0.37 mmol) were dissolved in 5 mL of dry DMF. A stream of argon was bubbled through the reaction mixture to expel oxygen. Tetrakis(acetonitrile)-copper(I) hexafluorophosphate (6.86 mg, 0.018 mmol), *N*-ethyldiisopropylamine (DIPEA) (103.4 mg, 0.8 mmol), and tris(benzyltriazolylmethyl)amine (TBTA), (10 mg, 0.018 mmol) were added under argon. The reaction mixture was sealed under argon and stirred overnight (24 h). Conversion was confirmed by TLC, (hexane/ethyl acetate, 5:1) with the product at R_f = 0.15 corresponding to the desired compound (**2a**). The solvent (DMF) was removed in vacuo and the residue was redissolved in a mixture of

hexane/ethyl acetate 8:1. The crude product was purified by column chromatography on silica gel, using hexane/ ethyl acetate (5:1) as the eluent. Removal of the solvent gave (**2a**) as colorless solid, 40 mg, yield 50%. Data for **2a**: $R_f = 0.15$ (hexane/ethyl acetate, 5:1). ^{1}H NMR (200 MHz, $CDCl_3$), (both diastereomers): δ 7.79, (d, 4H, phenyl-CH), 7.64, (s, 2H, triazole-H), 7.47−7.18 (m, 18H, phenyl-H), 5.56 (d, 4H, $-CH_2$-triazole), 4.93 (q, 2H, CH), 3.43 (d, 1H,^3J = 10.71 Hz, CH), 3.31 (d, 1H,^3J = 10.71 Hz, CH), 2.31 (m, 1H, CH), 1.62 (d,3H,^3J = 6.3 Hz, CH_3), 1.53 (d, 3H,^3J = 6.3 Hz, CH_3), 1.4 (m, 1H, CH), 1.31 (d, 3H,^3J = 6.3 Hz, CH_3), 1.05 (s, 9H, CH_3), 0.96 (d, 3H,^3J = 6.3 Hz, CH_3), 0.77 (s, 9H, CH_3), 0.55 (d, 3H,^3J = 6.5 Hz, CH_3), 0.22 (d, 3H,^3J = 6.6 Hz, CH_3). ^{13}C NMR (50 MHz, $CDCl_3$) (both diastereomers): δ 148.1 (triazole-C), 145.6 (phenyl-C), 141.8 (phenyl-C), 141.5 (phenyl-C), 133.5 (phenyl-C), 132.5 (phenyl-C), 130.9 (phenyl-CH), 130.8 (phenyl-CH), 130.4 (phenyl-CH), 128.8 (phenyl-CH), 128.1 (phenyl-CH), 127.9 (phenyl-CH) , 127.78 (phenyl-CH), 127.4 (phenyl-CH), 127.3 (phenyl-CH), 126.3 (phenyl-CH), 125.6 (d, phenyl-CH), 119.4 (triazole-CH), 83.1 (CH), 82.3 (CH), 72.3 (CH), 72.0 (CH), 61.14 (C), 60.7 (C), 54.1 ($-CH_2$-triazole), 54.0 ($-CH_2$-triazole), 31.90 (CH), 31.6 (CH), 28.3 (CH_3), 28.10 (CH_3), 24.6 (CH_3), 22.6 (CH_3), 22.2 (CH_3), 21.9 (CH_3), 21.1 (CH_3), 20.9 (CH_3).

5-(3-(1-(4-(1-(*tert*-Butyl-(2-methyl-1-phenylpropyl)aminooxy)-ethyl)benzyl)-1*H*-1,2,3-triazol-4-yl)propyl)-5-propylpyrimidine-2,4,6(1*H*,3*H*,5*H*)-trione (2b). 2,2,5-Trimethyl-3-(1′-*p*-azidomethylphenylethoxy)-4-phenyl-3-azahexane (**1b**)[31] (30 mg, 0.08 mmol) and 5-(pent-4-ynyl)-5-propylpyrimidine-2,4,6(1*H*,3*H*,5*H*)-trione (**4b**) (25 mg, 0.1 mmol) were reacted similar to compound **2a**, using tetrakis(acetonitrile)copper(I) hexafluorophosphate (3 mg, 0.008 mmol), *N*-ethyldiisopropylamine (DIPEA) (31 mg, 0.24 mmol), and tris(benzyltriazolylmethyl)amine (TBTA), (4 mg, 0.008 mmol) overnight (24 h). Conversion was confirmed by TLC, hexane/ethyl acetate, 1:1, $R_f = 0.4$. After purification by column chromatography using a gradient, starting with ethyl acetate/hexane = 1:1, gradually increasing to hexane/ethyl acetate 1:2, **2b** was obtained as a white solid: 40 mg, yield 80%.

Data for **2b**: $R_f = 0.4$ (hexane/ethyl acetate, 1:1). ^{1}H NMR (200 MHz, $CDCl_3$) (both diastereomers): δ 8.64 (d, 4H, phenyl-H), 7.45 (d, 2H, triazole-H), 7.32−7.13 (m, 16H, phenyl-H) 5.49,(d, 4H, $-CH_2$-triazole), 4.91 (q, 4H, CH), 3.43 (d, 1H, ^{3}J = 10.71 Hz, CH), 3.31 (d, 1H,^3J = 10.71 Hz, CH), 2.62 (s, 4H), 2.31 (m, 1H, CH), 2.0 − 1.89 (q, 8H, CH_2), 1.63−1.52 (m, 10H, CH_2), 1.29 − 1.2 (m, 6H, CH_3), 1.05 (s, 9H, CH_3), 0.96 (d, 3H,^3J = 6.3 Hz, CH_3), 0.77 (s, 9H, CH_3), 0.55 (d, 3H,^3J = 6.5 Hz, CH_3), 0.22 (d, 3H,^3J = 6.6 Hz, CH_3). ^{13}C NMR (50 MHz, $CDCl_3$) (both diastereomers): δ 173.04 (C═O), 149.49 (C═O), 145.01 (triazole-C), 140.93 (phenyl-C), 133.71 (phenyl-C), 133.14 (phenyl-C), 130.81 (phenyl-CH), 130.67 (phenyl-CH), 127.68−126.27 (m, phenyl-CH), 120.67 (triazole-CH), 83.17 (CH), 82.28 (CH), 72.12 (CH), 60.04 (**C**), 55.66($-CH_2$-triazole), 53.61($C_{barbituric\ acid}$), 31.38 (CH), 28.02 (**C**H_3), 27.87 (**C**H_3), 25.36 (CH_2), 24.63 (CH_2), 24.55 (CH_2), 24.51 (CH_3), 22.94 (CH_3), 22.05 (CH_3), 21.85 (CH_3), 20.89 (CH_3), 20.78 (CH_3), 18.15 (CH_2), 13.78 (CH_3).

4-(1-(*tert*-butyl-(2-methyl-1-phenylpropyl)aminooxy)ethyl)-benzyl 4-azidobenzoate (3c). 4-(1-(*tert*-Butyl(2-methyl-1-phenylpropyl)aminooxy)ethyl)benzyl 4-azidobenzoate (**3c**) was prepared analogous to a literature procedure[31] where an esterification reaction with potassium acetate was reported, which in our approach was replaced by potassium 4-azidobenzoate. 2,2,5-Trimethyl-3-(1′-*p*-chloromethylphenylethoxy)-4-phenyl-3-azahexane (**1a**) (50 mg, 0.133 mmol) was dissolved in HMPA (0.2 mL) and placed in a round-bottomed flask. Potassium 4-azidobenzoate (80 mg, 0.4 mmol) was added with a spatula, and the reaction was stirred for 48 h at room temperature. Conversion was screened by TLC (hexane/dichloromethane, 1:1, $R_f = 0.6$), although a complete consumption of **1a** did not occur. Formed salts and water-soluble side products were removed by extracting the reaction mixture with water/dichloromethane. The organic layer was separated and dried over $MgSO_4$, and the solvent was removed in vacuo. The crude product was purified by column chromatography, starting with pure hexane to remove residual HMPA, gradually increasing to hexane/dichloromethane = 1:1, furnishing 80%. Data for **3c**: $R_f = 0.6$ (hexane/dichloromethane, 1:1). ^{1}H NMR (200 MHz, $CDCl_3$) (both diastereomers): δ 8.08 (d, 4H, $J = 8.6$ Hz, phenyl-H) 7.46−7.04 (m, 22, phenyl-H) 5.35 (d, 4H, $-CH_2$-ester), 4.95 (q, 2H, CH), 3.43 (d, 1H,^3J = 10.71 Hz, CH), 3.32 (d, 1H,^3J = 10.71 Hz, CH), 2.35 (m, 1H, CH), 1.62 (d, 3H,^3J = 6.3 Hz, CH_3), 1.53 (d, 3H,^3J = 6.3 Hz, CH_3), 1.4 (m, 1H, CH), 1.31 (d, 3H,^3J = 6.3 Hz, CH_3), 1.05 (s, 9H, CH_3), 0.96 (d, 3H,^3J = 6.2 Hz, CH_3), 0.77 (s, 9H, CH_3), 0.55 (d, 3H,^3J = 6.4 Hz, CH_3), 0.22 (d, 3H,^3J = 6.4 Hz, CH_3). ^{13}C NMR: 165.59 (C═O), 145.85 (phenyl-C), 145.09 (phenyl-C), 142.10 (phenyl-C), 134.82 (phenyl-C), 134.8 (phenyl-C), 134.14 (phenyl-C), 130.50 (phenyl-CH), 130.85 (phenyl-CH), 128.02 (phenyl-CH), 127.36 (phenyl-CH), 127.21 (phenyl-CH), 126.32 (phenyl-CH), 83.21 (CH), 82.32 (CH), 72.12 (CH), 66.67 ($-CH_2$-ester), 66.65 ($-CH_2$-ester), 60.58 (C), 31.97 (CH), 31.66 (CH), 28.34 (CH_3), 28.27 (CH_3), 24.75 (CH_3), 23.10 (CH_3), 22.11 (CH_3), 21.91 (CH_3), 21.09 (CH_3), 21.02 (CH_3).

4-(1-(*tert*-Butyl-(2-methyl-1-phenylpropyl)aminooxy)ethyl)-benzyl 4-(4-Phenyl-1*H*-1,2,3-triazol-1-yl)benzoate (3a). 4-(1-(*tert*-Butyl(2-methyl-1-phenylpropyl)aminooxy)ethyl)benzyl 4-(4-phenyl-1*H*-1,2,3-triazol-1-yl)benzoate (**3a**) was prepared analogously to **2a**. Briefly, a solution of 4-(1-(*tert*-butyl(2-methyl-1-phenylpropyl)-aminooxy)ethyl)benzyl 4-azidobenzoate (**3c**) (60 mg, 0.12 mmol), ethynylbenzene (**4a**) (20 mg, 0.2 mmol), tetrakis(acetonitrile)copper-(I) hexafluorophosphate (4,5 mg, 0.012 mmol), *N*-ethyldiisopropylamine (DIPEA) (65 mg, 0.5 mmol) and tris(benzyltriazolylmethyl)-amine (TBTA), (6,4 mg, 0.02 mmol) were mixed in 5 mL of dry DMF under an atmosphere of argon and the reaction mixture was stirred overnight (24 h). TLC revealed a spot at $R_f = 0.2$ (hexane/chloroform, 1:1) corresponding to the desired product (**3a**). The solvent (DMF) was removed in vacuo and the crude product was purified by column chromatography on silica gel using a mixture of hexane/chloroform, 1:1 as the eluent. Removal of the solvent gave 56 mg of initiator **3a** as a solid substance: yield 80%. Data for **3a**: $R_f = 0.2$ (hexane/chloroform, 1:1). ^{1}H NMR (200 MHz, $CDCl_3$) (both diastereomers): δ 8.25 (d, 6H,^3J = 7.1, phenyl-H), 7.89 (m, 8H, phenyl-H), 7.49−7.17 (m, 24H, phenyl-H), 5.4 (d, 4H, $-CH_2$-ester), 4.97 (q, 2H, CH), 3.43 (d, 1H,^3J = 10.71 Hz, CH), 3.32 (d, 1H,^3J = 10.71 Hz, CH), 2.35 (m, 1H, CH), 1.62 (d, 3H,^3J = 6.3 Hz, CH_3), 1.53 (d, 3H,^3J = 6.3 Hz, CH_3), 1.4 (m, 1H, CH), 1.31 (d, 3H,^3J = 6.3 Hz, CH_3), 1.05 (s, 9H, CH_3), 0.96 (d, 3H,^3J = 6.2 Hz, CH_3), 0.77 (s, 9H, CH_3), 0.55 (d, 3H,^3J = 6.4 Hz, CH_3), 0.22 (d, 3H,^3J = 6.4 Hz, CH_3). ^{13}C NMR (50 MHz, $CDCl_3$) (both diastereomers): δ 165.25 (C═O), 148.72 (triazole-C), 146.00 (phenyl-C), 145.25 (phenyl-C), 142.08 (phenyl-C), 140.96 (phenyl-C), 134.54 (phenyl-C), 133.86 (phenyl-C), 131.45 (phenyl-CH), 130.83 (phenyl-CH), 130.17 (phenyl-CH), 129.80 (phenyl-CH), 128.93 (phenyl-CH), 128.62 (phenyl-CH), 128.14 (phenyl-CH), 127.35 (phenyl-CH), 127.27 (phenyl-CH), 126.36 (phenyl-CH), 125.85 (phenyl-CH), 119.75 (triazole-C), 117.82 (triazole-CH), 83.21 (CH) , 82.30 (CH), 72.11 (CH), 76.05 ($-CH_2$-ester), 60.59 (C), 31.95 (CH), 31.66 (CH), 28.33, 28.16 (CH_3) 24.74 (CH_3), 23.09 (CH_3), 22.12 (CH_3), 21.90 (CH_3), 21.07 (CH_3).

4-(1-(*tert*-Butyl-(2-methyl-1-phenylpropyl)aminooxy)ethyl)-benzyl 4-(4-(3-(2,4,6-Trioxo-5-propyl-hexahydropyrimidin-5-yl)-propyl)-1*H*-1,2,3-triazol-1-yl)benzoate (3b). 4-(1-(*tert*-Butyl(2-methyl-1-phenylpropyl)aminooxy)ethyl)benzyl 4-(4-(3-(2,4,6-trioxo-5-propyl-hexahydropyrimidin-5-yl)propyl)-1*H*-1,2,3-triazol-1-yl)benzoate (**3b**) was prepared according to the general method described for compound **2a**. 4-(1-(*tert*-Butyl(2-methyl-1-phenyl-propyl)aminooxy)ethyl)benzyl 4-azidobenzoate (**3c**) (100 mg, 0.2 mmol), 5-(pent-4-ynyl)-5-propylpyrimidine-2,4,6(1H,3H,5H)-trione (**4b**) (70 mg, 0.3 mmol), tetrakis(acetonitrile)copper(I) hexafluorophosphate (7.4 mg, 0.02 mmol), *N*-ethyldiisopropylamine (DIPEA) (103.4 mg, 0.8 mmol), and tris(benzyltriazolylmethyl)amine (TBTA) (10 mg, 0.02 mmol) were dissolved in 5 mL of DMF under an atmosphere of argon. The reaction mixture was sealed under argon and stirred overnight (24 h), indicating the formation of **3b** as a spot on TLC at $R_f = 0.3$ (hexane/ethyl acetate, 1:1). After removal of the solvent and purification by column chromatography starting a gradient with pure hexane, gradually increasing to hexane/

ethyl acetate, 1:1, **3b** was obtained as a yellowish solid substance: 115 mg, yield 90%. Data for **3b**: $R_f = 0.3$ (hexane/ethyl acetate, 1:1). ^{1}H NMR (200 MHz, $CDCl_3$) (both diastereomers): δ 8.76 (s, 4H, NH), 8.21 (d, 4H, $J = 8.5$ Hz, phenyl-H), 7.80 (t, 6H, $J = 5.5$ Hz, phenyl-H, triazole-H), 7.49−7.14 (m, 20H, phenyl-H), 5.38 (d, 4H, $-CH_2$-ester), 4.91, (q, 2H, CH), 3.43 (d, 1H,$^3J = 10.7$ Hz, CH), 3.31 (d, 1H,$^3J = 10.7$ Hz, CH), 2.78 (t, 4H $J = 7.3$ Hz, CH), 2.31 (m, 1H, CH), 2.16−1.91(q, 8H, CH_2), 1.63−1.52 (m, 10H, CH_2, CH_3), 1.29−1.2 (m, 6H, CH_2, CH_3) 1.05 (s, 9H, CH_3), 0.96 (d, 3H,$^3J = 6.3$ Hz, CH_3), 0.77 (s, 9H, CH_3), 0.55 (d, 3H,$^3J = 6.5$ Hz, CH_3), 0.22 (d, 3H,$^3J = 6.6$ Hz, CH_3). ^{13}C NMR (50 MHz, $CDCl_3$) (both diastereomers): δ 172.40 (C═O), 165.31 (C═O), 148.60 (triazole-C), 145.25 (phenyl-C), 142.08 (phenyl-C), 140.16 (phenyl-C), 134.54 (phenyl-C), 133.86 (phenyl-C), 131.42 (phenyl-CH), 130.85 (phenyl-CH), 130.02 (phenyl-CH), 128.15 (phenyl-CH), 127.27 (phenyl-CH), 126.38 (phenyl-CH), 119.75 (triazole-C), 118.92 (triazole-CH), 82.72 (CH), 82.33 (CH), 72.12 (CH), 69.38 (CH_2-ester), 67.05 (CH_2-ester), 60.59 (C), 56.44 (C-$5_{\text{barbituric acid}}$), 41.52 ($CH_2$), 37.83 ($CH_2$), 31.97 (CH), 31.67 (CH), 28.32 (CH_3), 27.25 (CH_3), 24.62 (CH_3), 23.10 (CH_3), 22.12 (CH_3), 21.03 (CH_3), 18.36 (CH_2), 13.87 (CH_3).

Synthesis of 4-(1-(*tert*-Butyl-(2-methyl-1-phenylpropyl)aminooxy)ethyl)benzyl 10,11-Dihydroxyundecanoate (3d). 2,2,5-Trimethyl-3-(1′-*p*-chloromethylphenylethoxy)-4-phenyl-3-azahexane (**1a**) (400 mg, 1.07 mmol) was dissolved in HMPA (6 mL) and placed in a round-bottomed flask, adding undec-10-ene carboxylic acid potassium salt (712 mg, 3.2 mmol). The mixture was stirred for 48 h at room temperature, screening the conversion by TLC (hexane/dichloromethane, 2:1, $R_f = 0.3$). Salts and water-soluble side products were removed by extracting the reaction mixture with a mixture of water and dichloromethane. The organic layer was separated from the aqueous phase, dried over $MgSO_4$ and the solvent was removed in vacuo. The crude product was purified by column chromatography on silica gel, starting with pure hexane to remove residual HMPA, gradually increasing to hexane/dichloromethane, 2:1), yielding 90% of 4-(1-(*tert*-butyl(2-methyl-1-phenylpropyl)aminooxy)ethyl)benzyl undec-10-enoate. ^{1}H NMR (200 MHz, $CDCl_3$) (both diastereomers): δ 7.42−7.05 (m, 18H, phenyl-H), 5.76 (m, 2H, = CH), 5.07 (d, 4H, $-CH_2$-ester), 4.89 (d, 4H, $J = 8$ Hz, $= CH_2$), 3.43 (d, 1H,$^3J = 10.71$ Hz, CH), 3.32 (d, 1H,$^3J = 10.71$ Hz, CH), 2.33 (m, 5H, CH, CH_2), 2.00 (q, 4H, CH_2), 1.55 (m, 11H, CH_3, CH_2, CH), 1.25 (s, 16H, CH_2), 1.05 (s, 9H, CH_3), 0.96 (d, 3H,$^3J = 6.2$ Hz, CH_3), 0.77 (s, 9H, CH_3), 0.55 (d, 3H,$^3J = 6.4$ Hz, CH_3), 0.22 (d, 3H,$^3J = 6.4$ Hz, CH_3). ^{13}C NMR (50 MHz, $CDCl_3$) (both diastereomers): δ 173.72 (C═O), 146.0 (phenyl-C), 145.3 (phenyl-C), 142.2 (phenyl-C), 142.1 (phenyl-C), 140.04 (phenyl-C) , 135.05 (═CH), 134.34 (phenyl-C), 130.95 (phenyl-CH), 130.86 (phenyl-CH), 127.12 (phenyl-CH), 126.28 (phenyl-CH), 114.13 ($=CH_2$), 83.20 (CH), 82.29 (CH), 72.16 (CH), 65.94 (CH_2-ester), 60.52 (C), 34.34 (CH_2), 33.76 (CH_2), 31.98 (CH), 31.68 (CH), 28.86 (C), 28.19 (C), 24.93 (CH_3), 24.22 (CH_3), 23.14 (CH_3), 22.09 (CH_3), 21.57 (CH_3), 20.55 (CH_3), 20.46(CH_3).

Further reaction of 4-(1-(*tert*-butyl(2-methyl-1-phenylpropyl)-aminooxy)ethyl)benzyl undec-10-enoate to the final product **3d** was achieved via a dihydroxylation reaction with OsO_4. For this reaction, a solution of 4-(1-(*tert*-butyl(2-methyl-1-phenylpropyl)aminooxy)-ethyl)benzyl undec-10-enoate (450 mg, 0.84 mmol) in dichloromethane and *N*-methylmorpholine-*N*-oxide (NMO) (237 mg, 2.0 mmol) was placed in a dry round-bottomed flask and subsequently rinsed with argon. Catalytic amounts of OsO_4 were added, and the reaction was stirred overnight. The formation of product (**3d**) was confirmed by TLC (chloroform/methanol, 20:1, $R_f = 0.45$). After the reaction had finished, a $NaHSO_4$ solution (10 w%) was added to the reaction mixture, and this solution was stirred for 30 min in order to destroy the remaining OsO_4. This mixture was filtered and the filtrate (organic and aqueous layer) were transferred to a separation funnel. The organic layer was separated, washed with brine, and dried with magnesium sulfate. Removal of the solvent by rotary evaporation yielded the desired product (**3d**), yield 75%, without the need for further purification. Data for **3d**: $R_f = 0.45$ (chloroform/methanol, 20:1). ^{1}H NMR (200 MHz, $CDCl_3$) (both diastereomers): δ 7.42−7.15 (m, 18H, phenyl-H), 4.12−3.16 (m, 10H, OH, CH, CH(OH)), 2.33 (t, 4H, $J = 7.5$ Hz, CH_2), 1.6−1.3 (m, 15H, CH_2), 2.00 (q, 4H, CH_2), 1.55 (m, 11H, CH_3, CH_2, CH), 1.25 (s, 16H, CH_2), 1.05 (s, 9H, CH_3), 0.96 (d, 3H,$^3J = 6.2$ Hz, CH_3), 0.77 (s, 9H, CH_3), 0.55 (d, 3H,$^3J = 6.4$ Hz, CH_3), 0.22 (d, 3H,$^3J = 6.4$ Hz, CH_3). ^{13}C NMR (50 MHz, $CDCl_3$): δ 169.08 (C═O), 146.0 (phenyl-C), 145.3 (phenyl-C), 142.2 (phenyl-C), 142.1 (phenyl-C), 140.04 (phenyl-C), 136.4, 135.7130.82 (phenyl-CH), 127.56 (phenyl-CH), 126.73 (phenyl-CH), 125.65 (phenyl-CH), 121.37, 121.09, 119.13, 109.52 (C−OH), 108.77 (C−OH), 82.59 (CH), 81.68 (CH), 71.53 (CH), 66.48 (CH_2-ester), 36.89 (CH_2), 35.08 (CH_2), 31.46 (CH), 31.17 (CH), 28.27 (C), 27.86 (C), 24.91 (CH_3), 24.22 (CH_3), 22.58 (CH_3), 22.08 CH_3), 21.59 (CH_3), 20.55 (CH_3), 20.46 (CH_3).

General Polymerization Procedure for Kinetic Investigations. Preparation of a **stock solution 1** of nitroxide in dry DMF: a 10 mL mensural flask was charged with 10 mg of 2,2,5-trimethyl-4-phenyl-3-azahexane-3-nitroxide. Dry DMF was added to give a final volume of 10 mL stock solution. The flask was sealed under argon and stored at 4 °C. Preparation of a **standard stock-solution 2** of ethyl methyl ketone in DMF: 5 g of ethyl-methyl-ketone were placed in a 100 mL mensural flask and DMF was added to yield a final volume of 100 mL. The flask was sealed and stored at 4 °C. Then, 0.8 mL of this solution was added to each sample after withdrawal, acting as the external standard for the subsequent GC measurements.

Polymerization Procedure. *N*-Isopropylacrylamide (*NIPAM*) (330 mg, 2.92 mmol) or *n*-butyl acrylate (*n*-BuA) (365 mg, 2.85 mmol) and one of the initiators, **1a**, **1b**, **2a**, **2b**, **3a**, **3b**, **3c** or **3d** (0.033 mmol), were dissolved in 1 mL of dry DMF and placed in a dry round-bottomed flask, rinsed with argon. 2,2,5-Trimethyl-4-phenyl-3-azahexane-3-nitroxide[31] (0.36 mg, 0.00165 mmol) was added by means of the **stock solution 1**: 0.36 mL of solution **1** was added by a syringe to the reaction mixture. Then 1.64 mL of dry DMF was added, yielding a final amount of 3 mL of dry DMF as the solvent. The flask was subjected to four freeze−thaw cycles and sealed under argon with a silicon seal. The so prepared reaction mixture was immersed in an oil bath at 120 °C. A first initial sample was drawn shortly after the flask has been immersed, to mark the start of the reaction and to be able to determine conversion with respect to this first sample. Then, 0.2 mL of the reaction mixture was withdrawn by with a 1 mL syringe, and placed in a glass vial; afterward 0.8 mL of the **standard-stock-solution 2** was added with a 1 mL syringe. Then 1 μL of this sample was injected into the SEC-54 column of a gas chromatograph. The course of the polymerization was followed by further sample withdrawals and analysis each 30−60 min. After the samples have been analyzed by GC, SEC measurements were carried out: all of the remaining sample volume was used for SEC measurements. The sample-solutions were transferred to a round-bottomed flask and evacuated under high vacuum in order to remove the solvent (DMF) and residual monomer. After all of the solvent had been removed, a brown vitreous solid was obtained which was redissolved again in 1 mL of dichloromethane. In the case of PNIPAM as the polymeric product, a precipitation by addition of 20 mL of diethyl ether was possible for further purification. The precipitated polymer was collected from the liquid organic layer by centrifugation, dried under high vacuum and redissolved in 1.5 mL of THF. This was filtrated and the sample solution was analyzed by SEC. However, poly-*N*-butyl acrylate (P-nBA) did not yield a precipitate upon the addition of methanol. The samples drawn from the *n*-BA polymerizations were treated identically to the PNIPAM samples, except for the purification by precipitation.

Preparation of Iron Oxide Nanoparticles Bearing the Diol Ligand 3d. The preparation of octylamine-covered γ-Fe_2O_3 nanoparticles (radius (DLS, TEM) = 8.6 nm)) was accomplished according to the literature.[38] IR (KBr pellet) ν (cm^{-1}): 3450 (−OH), 2926 ($-CH_3$, $-CH_2-$), 2857 ($-CH_3$, $-CH_2-$), 1623 ($-NH_2$), 1464 ($-CH_3$, $-CH_2-$). Ligand exchange using these nanoparticles was performed as follows: Surface modification reactions were performed according to the general protocol for ligand exchange

Scheme 2. Synthesis of the Nitroxide Initiators 1a, 1b, 2a, 2b, and 3a−3d (*N,N*-Dimethylformamide (DMF), Hexamethylphosphoric Acid Triamide (HMPA), Osmium Tetroxide (OsO_4))

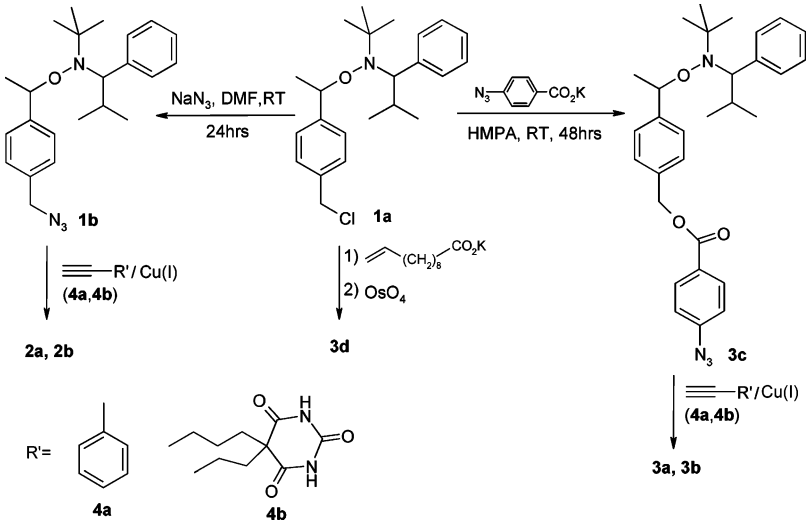

reactions of Rotello et al.[39] Thus, 50 mg of octylamine-covered stabilized NPs was dissolved in 30 mL of a 1:1 mixture of $CHCl_3$ and toluene. A second mixture was prepared consisting of 250 mg of diol ligand **3d** in a 1:1 mixture of chloroform and toluene. The ligand solution was added to the nanoparticle solution via a syringe and the reaction mixture was heated up to 50 °C under vigorous stirring for 2 days. After 48 h the exchange reaction has finished, resulting in surface modified nanoparticles. The particles were purified by repeated precipitation with dry methanol, centrifugation and resuspension in anhydrous toluene. Ligand exchange was proven by FTIR measurements, on the one hand by the absence of characteristic bands of the initially present octylamine-ligand, on the other hand by the presence of significant bands of the new functionalized ligand. Therefore, pure modified nanoparticles were dried under high vacuum and analyzed as KBr-pellets. **3d**-covered γ-Fe_2O_3 nanoparticles: IR (KBr-pellet) ν (cm^{-1}) 3431 (−OH), 2920 ($-CH_3$, $-CH_2-$), 2848 ($-CH_3$, $-CH_2-$), 1740 (-COOR), 1456 (−N−O−), 1260 (−OH), 1030 (two resonances for esters).

Surface-Initiated Polymerization from Iron Oxide Nanoparticles Using Surface-Bound Initiator 3d. A 10 mL round-bottomed flask was charged with an amount of nanoparticles that corresponded to 55 mg (0.1 mmol) of free initiator **3d**, as determined via TGA. 2,2,5-Trimethyl-4-phenyl-3-azahexane-3-nitroxide (1.1 mg, 0.005 mmol) and NIPAM (1 g, 8.85 mmol) were added. Then 5 mL of dry DMF was added as the solvent, and three freeze−thaw cycles were performed. The flask was sealed under argon and immersed in an oil bath pre-heated at a temperature of 150 °C. The reaction was stirred overnight and conversion was monitored via GC analysis, so that the reaction was finished at 90% of monomer conversion. The polymerization mixture was then allowed to cool down and the solvent (DMF) was removed in vacuo. The crude polymeric product was redissolved in few mL of dichloromethane and precipitated by pouring the crude polymer solution into 200 mL of diethyl ether. The polymeric product was collected by centrifugation, dried and the purification process by precipitation was repeated twice. The purified product was dried under high vacuum overnight. Characterization was done by TGA and DLS. The hybrid product was analyzed by TGA-measurements, showing a weight loss of 89.09 wt %. This indicates, that the nanoparticle−PNIPAM hybrid consists of 11 wt % iron oxide core and 89 wt % organic polymer shell. Furthermore, the superparamagnetic properties of the nanoparticle bound polymer were proven by a strong ferromagnet brought in close vicinity to the product as well as the free dispersibility on the absence of a magnetic field. Magnetic measurements using a superconducting interference device (SQUID) proved the superparamagnetic properties (data not shown here) Movement of the magnet resulted in the movement of the polymer powder.

Vacuum MALDI Mass Spectrometry. All measurements were performed using an Axima TOF^2 time-of-flight (TOF)/reflectron (RTOF) tandem mass spectrometer (Shimadzu Biotech Kratos Analytical, Manchester, U.K.) fitted with a nitrogen laser ($\lambda = 337$ nm, pulse width 4 ns) in the reflectron positive ion mode. A saturated solution of 2,5-dihydroxybenzoic acid (Sigma, St. Louis, MO) in water:methanol = 1:1 (v/v) was found to be the matrix of choice for this type of polymer samples. For sample preparation 0.5 μL of matrix solution was mixed 0.5 μL analyte solution (roughly 1 mg polymer per mL of water:methanol = 1:1 (v/v) solution) in a tube ("dried droplet technique") prior to sample deposition onto a brushed stainless steel target resulting in a homogeneous microcrystalline layer. Then 500 unselected single laser pulses were applied to obtain the individual mass spectra. Mass calibration was performed with a standard peptide mixture containing bradykinine fragment 1−7, angiotensin II, angiotensin I, human [Glu^1]-fibrinopeptide B, porcine *N*-acetyl-renine substrate tetradecapeptide, adrenocorticotropic hormone fragment 1−17, adrenocorticotropic hormone fragment 18−39 and adrenocorticotropic hormone fragment 7−38 (all: Sigma, St. Louis, MO). Typical mass accuracies obtained were within ± 0.3 Da with external calibration. A mass spectrometric resolution of 2200 to 5200 (fwhm) for all acquired mass spectra was obtained.

Results and Discussion

In order to generate a multitude of various nitroxide initiators, the chloromethyl-functionalized initiator **1a** was chosen as starting point for the synthesis of structural analogues. Because of the presence of the chloromethyl moiety, a strong potential for further functionalization,[31] utilizing simple nucleophilic substitution reactions is present. Our concept relied on the azido-functionalized initiator **1b** and **3c**, which served as central molecules for the Sharpless-type "click" reaction,[40−43] enabling the attachment of various functional groups via the triazole bridge, as shown in Scheme 2. However, the exchange of chlorine by this new chemical entity implies a change of the steric and electronic structure. To reveal whether there is an impact on the quality of the polymerization, induced by the triazole-bridge, various initiator-variants were tested via kinetic studies of the initiators **1a**, **1b**, **2a**, **and 2b**, as well as via the initiators **3a**−**3d**, where the binding of the functional moieties is achieved by an ester linkage to Hawker's initiator **1a**.

Synthesis of the Nitroxide Initiators. Starting from the well-known chloromethyl initiator **1a**,[30,37] a nucleophilic substitution using sodium azide led to the quantitative formation of the azidomethyl nitroxide **1b** (see Scheme 2). Since the CON

Table 1. Chemical and Physical Data for the Polymerization of *N*-Isopropylacrylamide (NIPAM) and *n*-Butyl Acrylate (*n*-BuA) Initiated from the Nitroxide Initiators 1a, 1b, 2a, 2b, and 3a−3d[a]

entry	polymer	initiator [I]	monomer [M]	$M_{n(GPC)}$ (g mol^{-1})	M_w/M_n	$M_{n,theor}$[c]	$M_{n,projected}$[d]	conversion
1	polymer **1**	**1a**	NIPAM	7300	1.20	7895	10 400	75%
2	polymer **2**	**1a**	*n*-BuA	7100	1.30	8274	11 196	73%
3		**1b**	NIPAM				10 439	<5%[b]
4	polymer **4**	**2a**	NIPAM	5000	1.15	9536	10 542	90%
5	polymer **5**	**2a**	*n*-BuA	6000	1.15	9140	11 304	80%
6		**2b**	NIPAM				10 646	<5%[b]
7	polymer **7**	**2b**	*n*-BuA	4900	1.08	6025	11 434	50%
8		**3c**	NIPAM				10 530	<5%[b]
9	polymer **9**	**3a**	NIPAM	5000	1.15	9429	10 632	88%
10	polymer **10**	**3b**	NIPAM	5400	1.15	7963	10 766	90%
11	polymer **11**	**3b**	*n*-BuA	6700	1.20	10 453	11 532	90%
12	polymer **12**	**3d**	NIPAM	5600	1.17	7522	10 585	75%

[a] The ratio of monomer/initiator in all reactions was fixed to [M]/[I] = 2.92/0.033. [b] Only formation of minor amounts of polymer [c] $M_{n,theor}$: Calculated molecular weight according to the monomer/initiator ratio, taking into account the conversion of monomer (as detected by GC). [d] $M_{n,proj}$: Calculated molecular weight according to monomer/initiator-ratio in the case of full conversion.

structure is supposed to cleave upon heating, transformations demanding harsh reaction conditions are unfavorable. Fortunately, the nucleophilic exchange reaction with *sodium azide* is sufficiently mild, the choice of DMF as the solvent drives the equilibrium toward the substituted product due to the poor solubility of the generated sodium chloride in DMF. Consequently, compound **1b** was obtained quantitatively after overnight stirring at room temperature, and without the need to add a phase-transfer catalyst or elevated temperatures, as it has been reported in literature.[31] In analogy to this reaction,[44] a direct nucleophilic substitution reaction of the chloromethyl initiator **1a** with potassium 4-azidobenzoate furnished the 4-azidobenzoyl-substituted initiator **3c** in 80% yield after 48 h reaction in HMPA at room temperature. With the azido-substituted nitroxides **1b** and **3c** in hand, azide/alkine-"click" reactions with the terminal alkynes **4a** and **4b** were conducted using tetrakis(acetonitrile)copper(I) hexafluorophosphate as the copper source, *N*-ethyldiisopropylamine as the base, and tris(benzyltriazolylmethyl)amine as the cocatalyst,[45] furnishing the corresponding "click"-products in high to moderate yields: **2a** (50%), **2b** (80%), **3a** (80%), and **3b** (90%). In all cases, the structure of the resulting products was proven by extensive NMR analysis (see NMR spectra in the Supporting Information). In order to introduce an alkyl diol moiety (required for the attachment to the iron oxide nanoparticles), reaction with ω-undecenoic acid and subsequent dihydroxylation reaction by use of OsO_4 furnished the initiator **3d** in an overall yield of 68% (two steps).

Polymerization of *N*-Isopropylacrylamide and *n*-Butyl Acrylate. The prepared initiators **1a**, **1b**, **2a**, and **2b** as well as **3a**−**3c** and **3d** were employed in the controlled polymerization of *N*-isopropylacrylamide (NIPAM) and *n*-butyl acrylate (*n*-BA). The kinetic progress of the polymerizations was monitored in order to understand (a) check the ability to employ a living polymerization of NIPAM and (b) to study the structural influence of initiator structure on the polymerization reaction. In all cases, the polymerization reactions were carried out under argon, performing freeze−pump−thaw cycles in order to remove oxygen, in a 10 mL round-bottomed flask in analogy to a literature-procedure,[31] but the amount of solvent, temperature, and reaction time were adjusted according to our own needs: the literature states a polymerization in bulk in the case of solvent monomers or only minor amounts of added DMF. However, the intended observation of the polymerization progress by determining the concentration of monomer demanded a solution of monomer. Furthermore, the reaction time mentioned in literature is about 48 h, opposed by our results that show conversion up to 60% and higher within 300 min at 120 °C. In a first set of experiments, the quality of control of the polymerization reaction (exemplified by M_n and M_w/M_n) was of interest (for data, see Table 1). In a second round, kinetic plots showing conversion vs polymerization time and molecular weight of the polymer vs monomer conversion were created to further check for the living behavior of the polymerization reaction. To this respect, the flask was immersed in a pre-heated oil bath at 120 °C and 0.2 mL portions of the reaction mixture were withdrawn at specific time intervals (20−120 min) and placed in a cooled glass vial, so that the polymerization was stopped.

Results of the polymerization of NIPAM and *n*-butyl acrylate (*n*-BuA) are shown in Table 1. Clearly, there are significant trends concerning the influence of the structure of the initiators on the polymerization reactions: (a) The azido-functionalized initiators **1b** and **3c** (entries 3 and 8) are not able to initiate a PNIPAM-polymerization. (b) The 4-chloromethyl initiator **1a** (entries 1 and 2) initiates both NIPAM and *n*-BuA in accordance with results reported by Hawker et al.[29,31] (c) Initiator **2a** (with a directly bound triazole moiety on the aryl-center of the initiating radical) initiates both NIPAM and *n*-BuA, yielding polymers with a low polydispersity (M_w/M_n = 1.15). (d) In contrast, initiator **2b** (entry 6 and 7), bearing the barbituric acid moiety via the directly triazole-linkage, could not initiate the polymerization of NIPAM, but those of *n*-BuA (M_w/M_n = 1.10). (e) Initiators **3a**, **3b**, and **3d**, bearing an ester bridge at the 4-methylenephenyl position of the initiating radical, however, showed good initiation quality toward NIPAM (**3a**, **3b**, and **3d**) and additionally *n*-BuA (**3b**), generating polymers with low polydispersities (ranging from 1.15 to 1.20).

Kinetic plots, depicting the monomer vs time course and the development of the molecular weight vs conversion of the polymerization reaction for the initiators **1a** (Figure 1, parts a and b) and initiator **2a** (Figure 1, parts c and d) are shown. In accordance with Hawkers's previous investigations, initiator **1a** yields a controlled radical polymerization (CRP) of NIPAM and *n*-BuA, as exemplified by the linear relationship between ln-[M_o/M] vs time and the correlation of the molecular weight vs conversion (Figure 1a,b). However, in some cases (as shown with *n*-BuA), there is an induction period of ∼100 min reproducible with high precision, before polymerization is starting. The reason for this effect remains unclear, despite an extensive purification of reagents and solvents. A similar relationship is observed with initiator **2a**, indicating a controlled growth up to ∼70% of conversion. However, albeit monomer conversion did continue, growth of chains stopped after they reached a molecular weight of 5000 g/mol in the case of

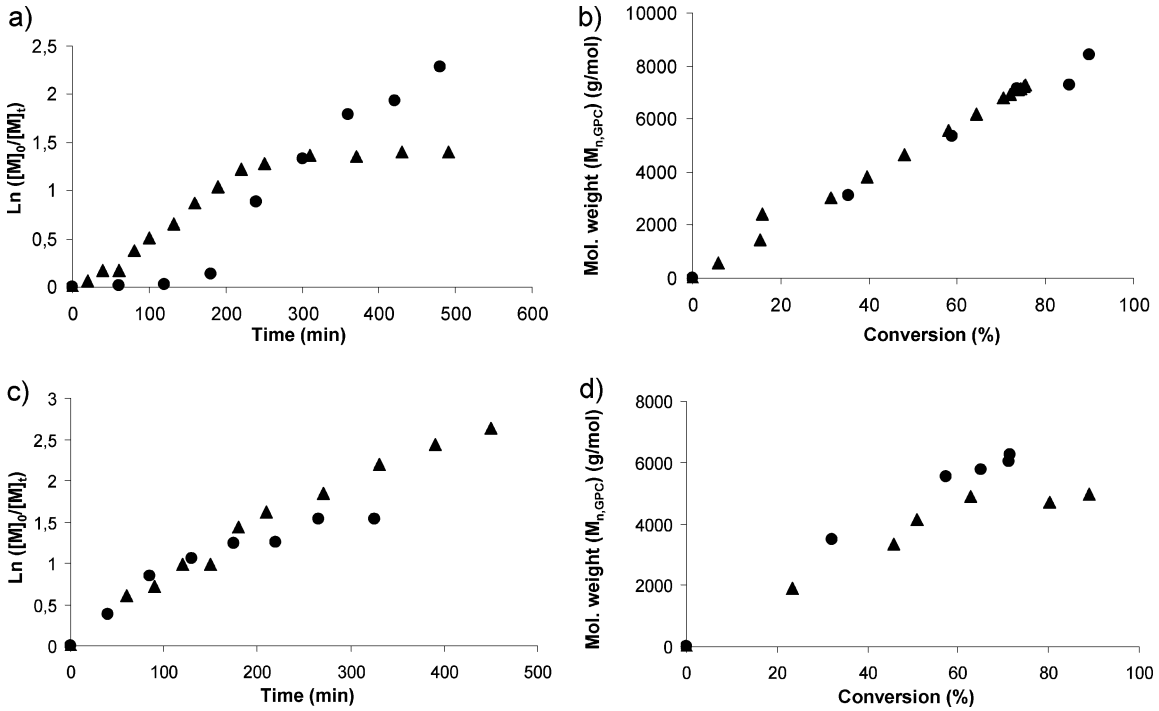

Figure 1. Kinetic results for the polymerization of initiator **1a** and **2a** with *N*-ispopropylacrylamide (NIPAM) and *n*-butyl acrylate (*n*-BuA) (a, b) kinetic plots and M_n vs conversion of polymerizations initiated with **1a** (▲, NIPAM; ●, *n*-BuA). (c, d) kinetic plots and M_n vs conversion of polymerizations initiated with **2a** (▲, NIPAM; ●, *n*-BuA).

NIPAM. The plot chain length vs conversion allows an evaluation of the quality of control in CRP: a CRP run projected at a chain length of 10 000 g/mol should yield a chain length of 5000 g/mol after 50% of monomer conversion. A good agreement is met for both monomers as displayed in Figure 1b. On the one hand, this confirms the validity of the kinetic model used to describe CRP for this polymerization;[46,47] on the other side, the results show that a derivatization of compound **1a** in the sense of a "click"-type reaction under formation of a triazole is possible.

The situation is more complex with the initiators **2b** and **3b**, both bearing a barbituric acid moiety, but differing in the nature of the linkage between the 4-phenyl-unit (**2b**: direct triazole linkage; **3b**: ester-linked triazole). Kinetic plots indicate polymerization of only *n*-BuA as monomer with **2b**, but surprisingly, both monomers (*n*-BuA and NIPAM) are polymerized in a controlled manner using initiator **3b**. Kinetic plots are depicted in Figure 2, parts a and b (initiator **2b**/*n*-BuA), and Figure 2, parts c and d (initiator **3b**/*n*-BuA and NIPAM). Conversion of initiator **2b** with NIPAM remains below the measurable amount of 5%. Bearing in mind the challenge NIPAM imposed on controlled radical polymerization techniques such as ATRP[14−26] and NMP[27−36] this result came not as a surprise: NIPAM is known to be a difficult monomer for CRP,[48] as ATRP and NMP both represent techniques that are difficult in polymerizing NIPAM with control. However, a detailed reasoning of this quite unexpected behavior can be discussed in terms of stereoelectronic and—most of all—hydrogen-bonding effects (vide infra). Finally, Figure 3 depicts the kinetic results for initiator **3d** with NIPAM as monomer, depicting a linear relationship between $\ln[M_o/M]$ vs time and the correlation of the molecular weight vs conversion, indicative of a highly controlled polymerization process ($M_w/M_n = 1.17$, after 75% conversion).

In order to understand the different behavior of initiators **2a**/**2b** (both bearing a directly bound triazole moiety, with initiator **2b** additionally showing a bound barbituric acid moiety) and the initiators **3a**/**3b** (attaching the phenyl and barbituric acid moieties via an ester/triazole linkage), two different effects were taken into account: as described by various authors,[49−52] the rate of C−O bond cleavage within the nitroxides is dependent on stereo-electronic factors, resulting from the dissociation energy of the C−O−N bond. Thus, substituents exerting an electronic-withdrawing effect at the 4′-position usually lead to an acceleration of rate of homolysis k_d in the equilibrium between the dissociated and the covalent form. The electronic influence in para-substituted compounds of the structure TEMPO−CH−$(CH_3)C_6H_5X$ on the homolysis rate constants has been described by Studer et al.[53] decreasing in the order $X =$ (*p*-MeO_2C) > *p*-Br > *p*-H > *p*-Me > *p*-MeO. However, ether moieties on the 4′-position of the styryl moiety of TIPNO-based initiators for NMP have been described to actively promote a CRP-process, although not with NIPAM as monomer.[54] The structure of the residues at the 4′-position in the (TIPNO-based) initiators **2a**/**2b** and **3a**/**3b** is different in terms of their electronic influence: whereas a strongly electron-withdrawing ester moiety is present in the initiators **3a** and **3b**, a less electronic withdrawing group is present in form of the triazole moiety in the compounds **2a** and **2b**. This may explain the observation that **3a** acts as an initiator for the CRP of *n*-BuA and NIPAM, whereas the structurally homologous initiator **2a** acts as initiator for the CRP of the "easier" monomer *n*-BuA only. However, in addition to stereoelectronic effects, several authors have described hydrogen-bonding effects as another major factor influencing the reactivity of the C−O bond cleavage in nitroxides.[55−58] Effects of hydrogen bonds, structurally present in the nitroxide moiety can lead to an enhanced cleavage of the C−O bond via a stabilization of the resulting by an intramolecular hydrogen bond.[53] Thus, not the rate of cleavage is increased, but the rate of recombination is reduced by this hydrogen-bonding effect. In the case of the initiators **2b** and **3b**, however, the hydrogen-bonding effects can result from moieties within the styryl fragment, instead of the nitroxide fragment of the initiating moiety. Therefore, a stabilization of

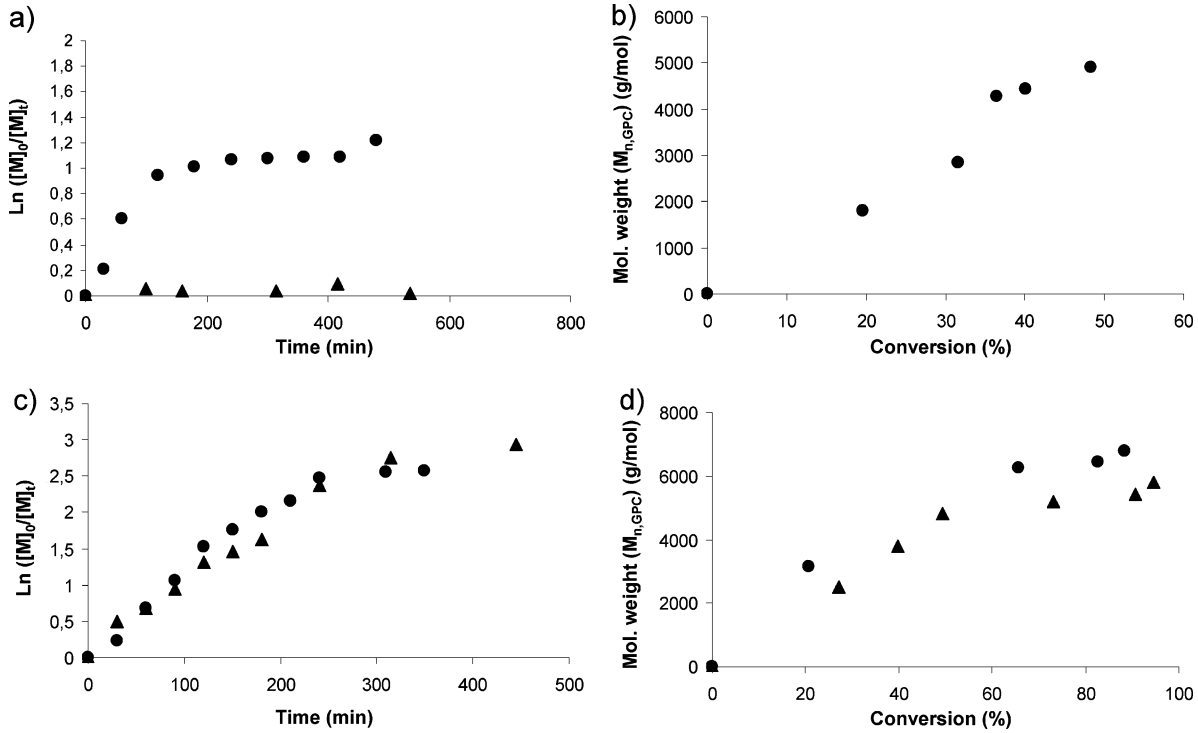

Figure 2. Kinetic results for the polymerization of initiator **2b** and **3b** with *N*-ispropylacrylamide (NIPAM) and *n*-butyl acrylate (*n*-BuA) (a, b) kinetic plots and M_n vs conversion of polymerizations initiated with **2b** (▲, NIPAM; ●, *n*-BuA). (c, d) kinetic plots and M_n vs conversion of polymerizations initiated with **3b** (▲, NIPAM; ●, *n*-BuA).

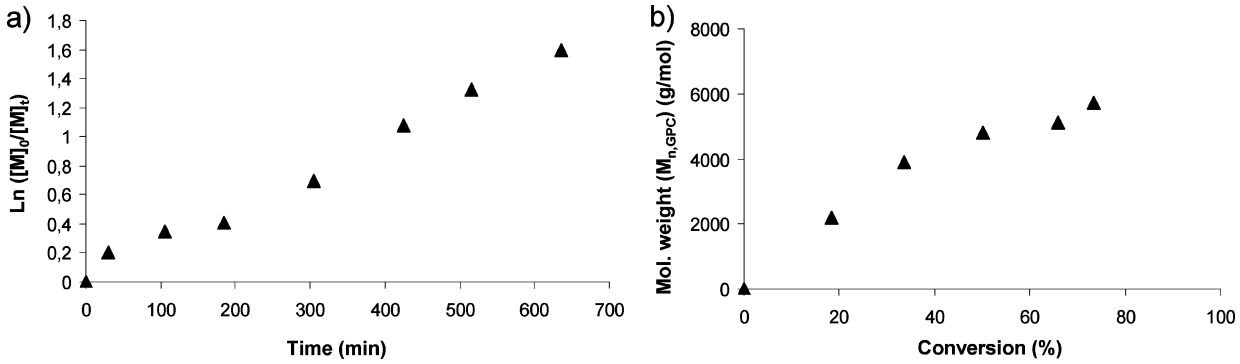

Figure 3. Kinetic results for the polymerization of initiator **3d** with *N*-ispopropylacrylamide (NIPAM) (a) kinetic plots and (b) M_n vs conversion of polymerizations initiated with **3d** (▲, NIPAM).

the styryl radical by the hydrogen bond would lead to a deactivation of the propagating radical, thus lowering its efficiency for polymerizing monomers such as NIPAM, which traditionally require stronger radicals for activation than *n*-BuA.

In order to evaluate the hydrogen-bonding effect in compounds **2b** and **3b**, geometry optimization calculations were performed with three-dimensional models (see Figure 4, parts a and b). A molecular mechanics calculation using an MM2 force field was performed, to calculate the steric energy of two conformations of the molecules **2b** and **3b** (see Figure 4, parts a and b, respectively). First, a conformation without additional manipulation of the structure was subjected to such a calculation, as to have a referential energy and a three-dimensional appearance for comparison. Then the structure was intentionally manipulated wherein the benzylic radical center was brought into close vicinity to an acidic hydrogen, and another geometry optimization was carried out. This manipulation was done stepwise, by moving the moiety bearing the acidic hydrogens closer to the benzylic position in small increments, because a severe manipulation at once may lead to physically unreasonable conformations. It was tested whether the provided, forced structure would lead to a local reasonable energy minimum, corresponding to a stable conformation that would generally make an interaction of the radical and an acidic hydrogen possible. Since no quantum mechanics are included and no electronic states are taken into account, MM2 is incapable to calculate the formation of bonds (covalent or associative); therefore, the hydrogen bond and its potential interaction with a radical cannot be calculated. Initiator **3b** yielded the largest distance (6.3 angström) between an acidic hydrogen and the benzylic radical center. This is due to the succession of three sp^2-hybridized structures (ester, aromatic ring and triazole) in the molecule, creating a rigid, planar linking unit between the barbituric acid and the reactive center. Initiator **2b** is more flexible due to the lack of this linker, and the flexible chain between barbituric acid and the triazole, as well as the CH_2 group between triazole and styryl moiety, enables us to adopt a globular structure, holding the potential for H-bonding (3.1 Å). Therefore, the formation of an intramolecular hydrogen bond is possible in initiator **2b**, but is highly unlikely in initiator **3b**, due to the rigid segment of the additional, aromatic moiety, explaining the reduced initiating quality of initiator **2b** with

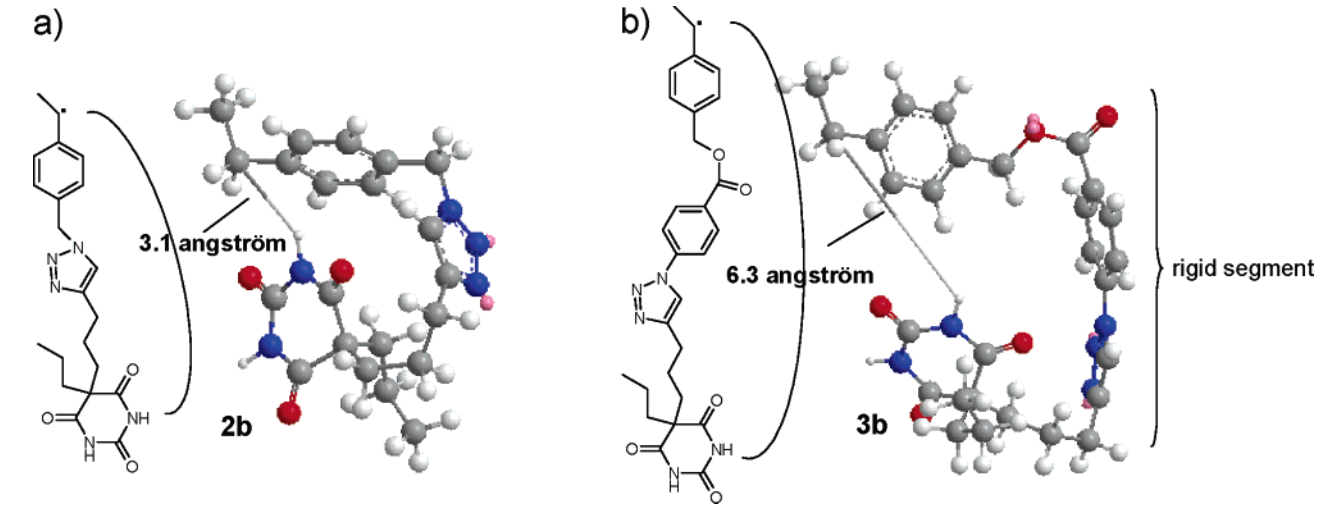

Figure 4. MMR-force-field distance evaluation of the initiators (a) **2b** and (b) **3b**.

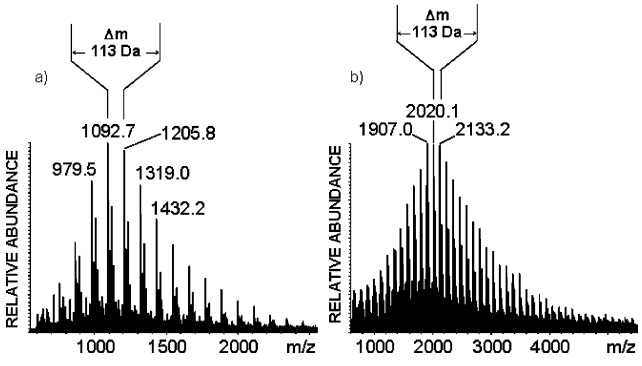

Figure 5. MALDI spectra of (a) polymer **4** (initiated by **2a**/NIPAM) and (b) polymer **10** (initiated by **3b**/NIPAM).

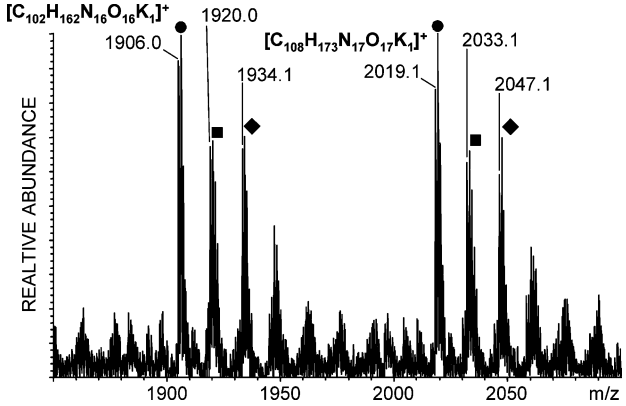

Figure 6. Detail of the MALDI-spectrum of polymer **10** (initiated by **3b**/*N*-isopropylacrylamide (NIPAM)).

respect to NIPAM. Obviously, initiator **2b** is still sufficiently reactive to allow the CRP of *n*-BuA. Initiator **3b**, more active due to the impossibility of inhibition of the radical center in contrast displays a much higher reactivity and, therefore, a CRP of the monomers *n*-BuA and NIPAM.

Vacuum MALDI Mass Spectrometry. Since MALDI TOF mass spectrometry[59] has been demonstrated in the past to represent a useful method for the analysis of telechelic PNIPAM polymers,[9,13,36] this technique was applied in this investigation, too. Figure 5a and 5b show the mass spectra for polymer **4** (initiated by **2a**/NIPAM) and polymer **10** (initiated by **3b**/NIPAM). Both mass spectra show the series for polymer **4** with $m/z = 1092.7 \pm n \times 113.1$ (NIPAM), corresponding to $[M + 2Na - H]^+$ (calcd: 1092,7 $C_{61}H_{93}N_9O_6Na_2$) and polymer **10** with $m/z = 2019.1 \pm n \times 113.1$ (NIPAM), corresponding interestingly to $[M + K]^+$, (calcd: 2019.3 $C_{108}H_{173}N_{17}O_{17}K$). Therefore, the main signals are attributed to the polymers **4** and **10** bearing both end group moieties, stemming from the initiators **2a** and **3b** respectively. The presence of the potassium adduct ions ($[M+K]^+$) in polymer **10** clearly results from the use of potassium salts in the preparation of the initiator **3b**, in contrast to the initiator **2a**, where only the sodium adduct ion series ($[M + 2Na - H]^+$ are visible. In both cases, the maximum of the respective curves does not correspond to the values obtained via SEC—hinting at a favored desorption/ionization of the lower molecular weight oligomers. Expansion of the MALDI-spectrum of polymer **10** (see Figure 6) however reveals two other series with a repeating unit of $\Delta m = 113.16$ (NIPAM), which could not be assigned to any possible structure. Summed up, the MALDI investigations clearly demonstrate the presence of the telechelic polymers, proving the presence of both end group moieties resulting form the initiating nitroxide, as expected for the CRP process on the basis of the nitroxide mediated polymerization of NIPAM.

Magnetic Nanoparticles with a NIPAM Shell via "Grafting-from" Methods. On the basis of the promising results with respect to the controlled radical polymerization of NIPAM, initiated by the dihydroxyalkyl initiator **3d**, a surface initiated process was investigated (see Figure 7). Since it is well-known that NMP from planar surfaces using an initiator[44,60] structurally related to TEMPO or TIPNO proceed in a controlled manner, generating uniformly grafted PNIPAM on homogeneous and patterned surfaces, we have studied the NMP process from the γ-iron oxide nanoparticles. Initiator **3d** bears a 1,2-diol moiety, which enables the attachment onto iron oxide, as studied by Rotello et al.[39] via related dihydroxy compounds. Therefore, starting from γ-iron oxide nanoparticles, covered with octylamine moietes, ligand exchange was effected by providing an excess of ligand **3d** in a chloroform/toluene mixture at 50 °C and 48 h. The particles were purified by repeated precipitation with dry methanol, centrifugation and resuspension in anhydrous toluene. Ligand exchange leading to **NP1** was proven by FTIR measurements, on the one hand by the absence of characteristic bands of the initially present octylamine ligand, on the other hand by the appearance of significant bands of the new functionalized ligand **3d** (see Experimental Section). The resulting nanoparticles (**NP1**) were then used to initiate the controlled polymerization of NIPAM, yielding iron oxide nanoparticles coated with a thermo responsive organic shell. However, an initial attempt to polymerize NIPAM using these

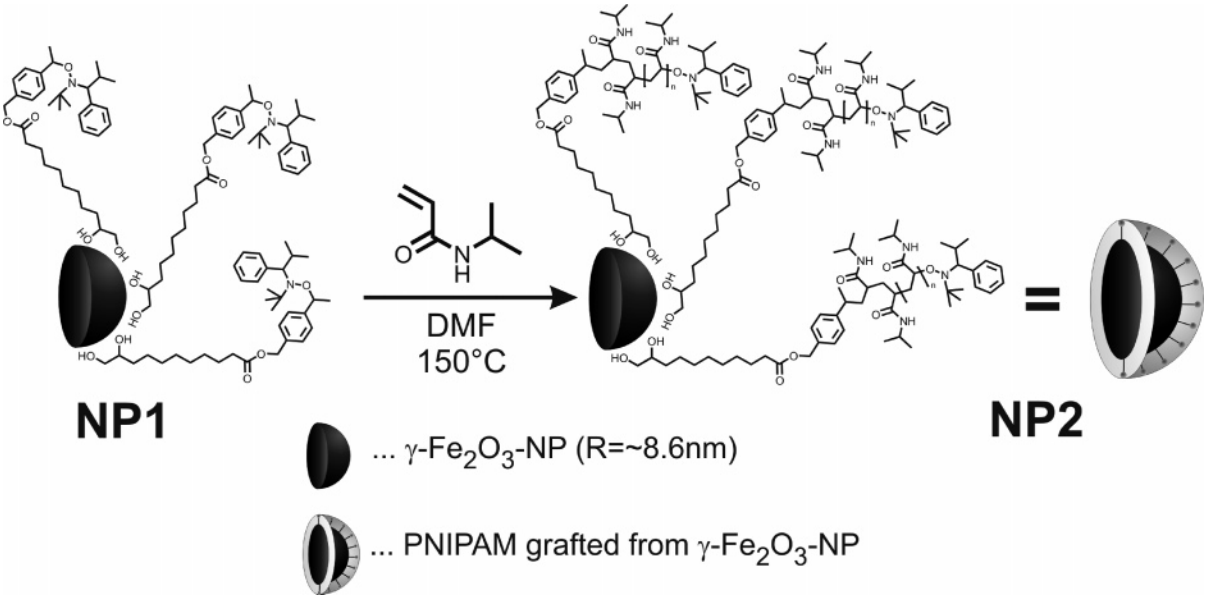

Figure 7. "Grafting-from" of NIPAM from the surface of γ-Fe_2O_3 nanoparticles with attached ligand **3d**.

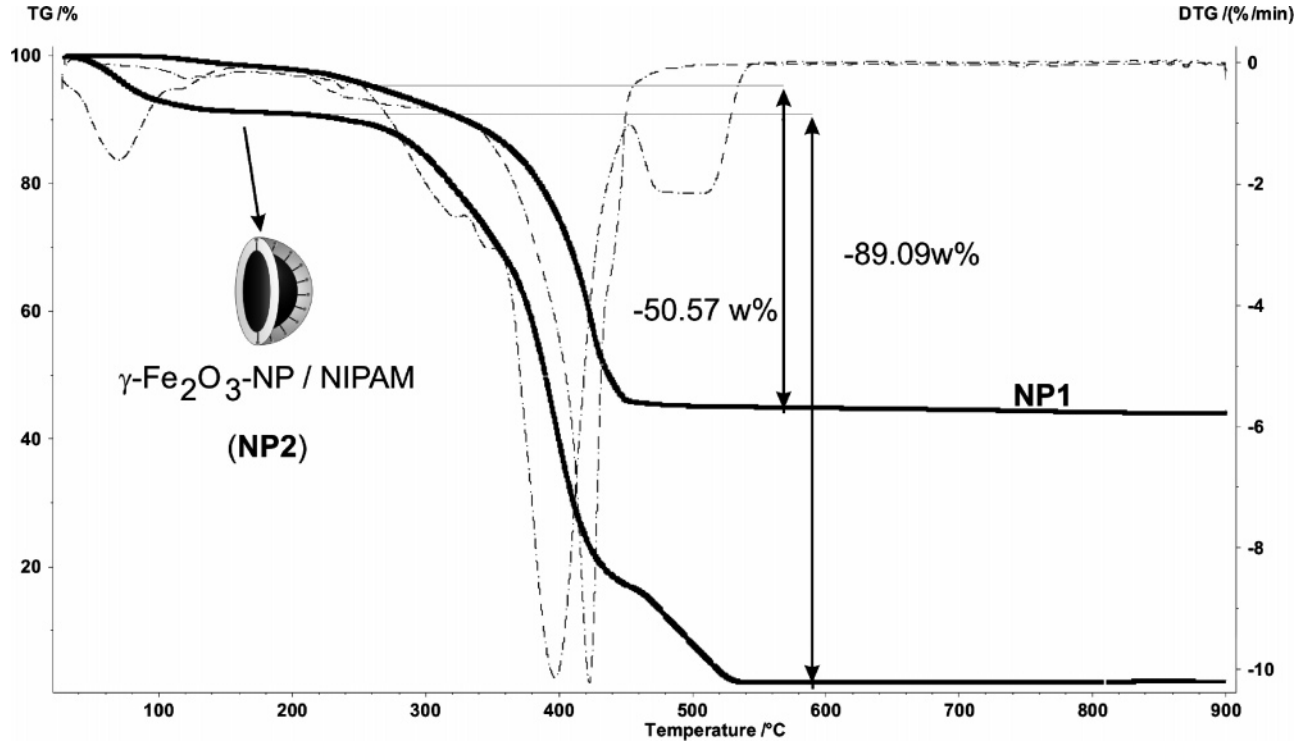

Figure 8. Thermogravimetric analysis (TGA) of (a) γ-Fe_2O_3-nanoparticles with attached ligand **3d** (**NP1**) and (b) γ-Fe_2O_3-nanoparticles with grafted PNIPAM (**NP2**) (M_n = 5600 g mol^{-1}; M_w/M_n = 1.20).

nanoparticles, bearing the immobilized receptor **3d** at a temperature of 120 °C failed, but increasing the reaction temperature to 150 °C yielded 90% of monomer conversion after overnight stirring. The resulting nanoparticles (**NP2**), bearing grafted PNIPAM were characterized by TGA (see Figure 8), in order to quantify the amount of immobilized polymer. The analysis revealed a relative weight loss of 89%, correlated with data obtained from the non-nanoparticle bound polymer: SEC measurements of this polymeric product yielded a molecular weight of 5600 g/mol. Since the polymerization run using the surface bound initiator **3d** was projected at a molecular weight of 10000 g/mol, the surface bound PNIPAM chains are assumed to hold approximately the same molecular weight as polymer **12** (see Table 1). Since other parameters such as the binding area per ligand, and total surface area of the nanoparticles are known[61] the total amount of ligands can be calculated. Indeed, a theoretical weight loss (when taking 5600 g/mol as the molecular weight of the surface bound ligand) of 90% has been calculated.

Conclusion

Summed up, we have demonstrated a new approach toward telechelic poly(*N*-isopropylacrylamide)s via an NMP process, initiated by functional nitroxides on the basis of TIPNO derivatives. A simple approach toward various initiators, based on a combination of nucleophilic substitution steps and subsequent azide/alkine "click" reactions generated several TIPNO initiators, modified at their styryl end. Kinetic investigations with these initiators revealed a strong influence of the functional groups attached to the styryl part, with the directly triazole-

bound initiators as the poorest initiators toward NIPAM as the monomer. The presence of an additional ester moiety between the styryl part of the initiator and the triazole linkage lead to a highly controlled process, proving the incorporation of end groups into the telechelic PNIPAM polymer, as demonstrated by MALDI mass spectrometric analysis. Intermolecular hydrogen-bonding effects of the present hydrogen donor moieties rather than purely electronic effects can be made responsible for the differing initiating quality of the structurally related initiators, as proven by molecular mechanics calculations. The versatility of the process was demonstrated by a grafting-from approach of PNIPAM from the surface of γ-Fe_2O_3 nanoparticles, generating superparamagnetic core/shell nanoparticles with a defined PNIPAM-shell. The approach in general opens an easy access toward functionalized telechelic PNIPAM polymers with defined chain length and a highly defined, functional end group chemistry.

Acknowledgment. We would like to express thanks for a grant from the Austrian Science Foundation FWF (Project FWF 18740-B03) for financial support.

Supporting Information Available: Text giving a detailed calculation of PNIPAM on the nanoparticle surface, a table of structural data, and figures showing NMR spectra of the compounds **1a**, **1b**, **2a**, **2b**, and **3a**−**3d** and TEM of the iron oxide nanoparticles and the material with the grafted PNIPAM. This material is available free of charge via the Internet at http://pubs.acs.org.

References and Notes

(1) Schild, H. G. *Prog. Polym. Sci.* **1992**, *17*, 163−249.
(2) Jesorka, A.; Markström, M.; Orwar, O. *Langmuir* **2005**, *21*, 1230−1237.
(3) Idota, N.; Kikuchi, A.; Kobayashi, J.; Akiyama, Y.; Sakai, K.; Okano, T. *Langmuir* **2006**, *22*, 425−430.
(4) Ito, Y. *Biomaterials* **1999**, *20*, 2333−2342.
(5) Kikuchi, A.; Okano, T. *Prog. Polym. Sci.* **2002**, *27*, 1165−1193.
(6) Scales, C. W.; Convertine, A. J.; McCormick, C. L. *Biomacromolecules* **2006**, *7*, 1389−1392.
(7) Convertine, A. J.; Ayres, N.; Scales, C. W.; Lowe, A. B.; McCormick, C. L. *Biomacromolecules* **2004**, *5*, 1177−1180.
(8) Kujawa, P.; Segui, F.; Shaban, S.; Diab, C.; Okada, Y.; Tanaka, F.; Winnik, F. M. *Macromolecules* **2006**, *39*, 341−348.
(9) Schilli, C.; Lanzendörfer, M. G.; Müller, A. E. *Macromolecules* **2002**, *35*, 6819−6827.
(10) Savariar, E. N.; Thayumanavan, S. *J. Polym. Sci.:Part A: Polym. Chem.* **2004**, *42*, 6340−6345.
(11) Ganachaud, F.; Monteiro, M. J.; Gilbert, R. G.; Dourges, M.-A.; Thang, S. H.; Rizzardo, E. *Macromolecules* **2000**, *33*, 6738−6745.
(12) Carter, S.; Rimmer, S.; Sturdy, A.; Webb, M. *Macromol. Biosci.* **2005**, *5*, 373−378.
(13) Ray, B.; Isobe, Y.; Matsumoto, K.; Habaue, S.; Okamoto, Y.; Kamigaito, M.; Sawamoto, M. *Macromolecules* **2004**, *37*, 1702−1710.
(14) Xia, Y.; Burke, N. A. D.; Stöver, H. D. H. *Macromolecules* **2006**, *39*, 2275−2283.
(15) Li, G.; Shi, L.; An, Y.; Zhang, W.; Ma, R. *Polymer* **2006**, *47*, 4581−4587.
(16) Bontempo, D.; Li, R. C.; Ly, T.; Brubaker, C. E.; Maynard, H. D. *Chem. Commun.* **2005**, 4702−4707.
(17) Couet, J.; Biesalski, M. *Macromolecules* **2006**, *39*, 7258−7268.
(18) Kizhakkedathu, J. N.; Norris-Jones, R.; Brooks, D. E. *Macromolecules* **2004**, *37*, 734−743.
(19) Li, C.; Gunari, N.; Fischer, K.; Janshoff, A.; Schmidt, M. *Angew. Chem., Int. Ed.* **2004**, *43*, 1101−1104.
(20) Xu, F. J.; Zhong, S: P.; Yung, L. Y. L.; Kang, E. T.; Neoh, K. G. *Biomacromolecules* **2004**, *5*, 2392−2403.
(21) Farhan, T.; Huck, W. T. S. *Europ. Polym. J.* **2004**, *40*, 1599−1604.
(22) Bontempo, D.; Maynard, H. D. *J. Am. Chem. Soc.* **2005**, *127*, 6508−6509.
(23) Liu, Y.; Klep, V.; Luzinov, I. *J. Am. Chem. Soc.* **2006**, *128*, 8106−8107.
(24) Wang, X.; Tu, H.; Braun, P. V.; Bohn, P. W. *Langmuir* **2006**, *22*, 817−823.
(25) Skrabania, K.; Kristen, J.; Laschewsky, A.; Akdemir, Ö.; Hoth, A.; Lutz, J.-F. *Langmuir* **2006**, ASAP.
(26) Kizhakkedathu, J. N.; Kumar, K. R.; Goodman, D.; Brooks, D. E. *Polymer* **2004**, *45*, 7471−7489.
(27) Hawker, C. J. *Acc. Chem. Res.* **1997**, *30*, 373−382.
(28) Hawker, C: J.; Bosman, A. W.; Harth, E. *Chem. Rev.* **2001**, *101*, 3661−3688.
(29) Harth, E.; Bosman, A.; Benoit, D.; Helms, B.; Frechet, J. M. J.; Hawker, C. J. *Macromol. Symp.* **2001**, *174*, 85−92.
(30) Benoit, D.; Chaplinski, V.; Braslau, R.; Hawker, C. J. *J. Am. Chem. Soc.* **1999**, *121*, 3904−3920.
(31) Bosman, A. W.; Vestberg, R.; Heumann, A.; Frechet, J. M. J.; Hawker, C. J. *J. Am. Chem. Soc.* **2003**, *125*, 715−728.
(32) Savariar, E. N.; Thayumanavan, S. *J. Polym. Sci., Part A: Polym. Chem.* **2004**, *42*, 6340−6345.
(33) Gibbons, O.; Carroll, W. M.; Aldabbagh, F.; Yamada, B. *J. Polym. Sci., Part A: Polym. Chem.* **2006**, *44*, 6410−6418.
(34) Li, J.; Chen, X.; Chang, Y.-C. *Langmuir* **2005**, *21*, 9562−9567.
(35) Kuroda, K.; Swager, T. M. *Macromolecules* **2004**, *37*, 716−724.
(36) Schulte, T.; Siegenthaler, K. O.; Liftmann, H.; Letzel, M.; Studer, A. *Macromolecules* **2005**, *38*, 6833−6840.
(37) Dao, J.; Benoit, D.; Hawker, C. J. *J. Polym. Sci.* **1998**, *36*, 2161−2167.
(38) Rockenberger, J.; Scher, E. C.; Alivisatos, A. P. *J. Am. Chem. Soc.* **1999**, *121*, 11595−11596.
(39) Boal, A. K.; Das, K.; Gray, M.; Rotello, V. M. *Chem. Mater.* **2002**, *14*, 2628−2636.
(40) Binder, W. H.; Sachsenhofer, R. *Macromol. Rapid Commun.* **2007**, *28*, 15−54.
(41) Binder, W. H.; Kluger, C. *Curr. Org. Chem.* **2006**, *10*, 1791−1815.
(42) Maarseveen, J. H.; Hiemstra, H.; Bock, V. D. *Eur. J. Org. Chem.* **2006**, 51−68.
(43) Sharpless, K. B.; Finn, M. G.; Kolb, H. C. *Angew. Chem., Int. Ed.* **2001**, *40*, 2004 -2021.
(44) von Werne, T. A.; Germack, D. S.; Hagberg, E. C.; Cheares, V. V.; Hawker, C. J.; Carter, K. R. *J. Am. Chem. Soc.* **2003**, *125*, 3831−3838.
(45) Chan, T. R.; Hilgraf, R.; Sharpless, K. B.; Fokin, V. V. *Org. Lett.* **2004**, *6*, 2853−2855.
(46) Fischer, H. *Chem. Rev.* **2001**, *101*, 3581−3610.
(47) Tang, W.; Fukuda, T.; Matyjaszewski, K. *Macromolecules* **2006**, *39*, 4332−4337.
(48) Teodorescu, M.; Matyaszewski, K. *Macromolecules* **1999**, *32*, 4826−4831.
(49) Marque, S.; Le Mercier, C.; Tordo, P.; Fischer, H. *Macromolecules* **2000**, *33*, 4403−4410.
(50) Studer, A.; Harms, K.; Knoop, C.; Müller, C.; Schulte, T. *Macromolecules* **2004**, *37*, 27−34.
(51) Bertin, D.; Gigmes, D.; Marque, S. R. A.; Tordo, P. *Macromolecules* **2005**, *38*, 2638−2650.
(52) Wetter, C.; Gierlich, J.; Knoop, C. A.; Müller, C.; Schulte, T.; Studer, A. *Chem.—Eur. J.* **2004**, *10*, 1156−1166.
(53) Marque, S.; Fischer, H.; Baier, E.; Studer, A. *J. Org. Chem.* **2001**, *66*, 1146−1156.
(54) Lohmeijer, B. G. G.; Schubert, U. S. *J. Polym. Sci.* **2005**, *43*, 6331−6344.
(55) Franchi, P.; Lucarini, M.; Pedrielli, P.; Pedulli, G. F. *ChemPhysChem* **2002**, *3*, 789−793.
(56) Goto, A.; Kwak, Y.; Yoshikawa, C.; Tsujii, Y.; Sugiura, Y.; Fukuda, T. *Macromolecules* **2002**, *35*, 3520−3525.
(57) Harth, E.; Van Horn, B.; Hawker, C. J. *Chem. Commun.* **2001**, 823−824.
(58) Knoop, C: A.; Studer, A. *J. Am. Chem. Soc.* **2003**, *125*, 16327−16333.
(59) Experimental details, see: Belgacem, O.; Bowdler, A.; Brookhouse, I.; Brancia, F. L.; Raptakis, E. *Rapid Commun. Mass Spectrom.* **2006**, *20*, 1653−1160.
(60) Hutchison, J. B.; Stark, P. F.; Hawker, C. J.; Anseth, K. S. *Chem. Mater.* **2005**, *17*, 4789−4797.
(61) Weinstabl, H. C.; Diploma Thesis, TU-Vienna, Vienna, 2006.

MA0628376